



Molecular Crystals and Liquid Crystals

Publication details, including instructions for authors and subscription information:

<http://www.tandfonline.com/loi/gmcl20>

Real-Time Optical Information Processing Through the Use of Low-Saturable Absorption in Bacteriorhodopsin Films

Nikolai Burykin^a, Dmitriy Stepanchikov^b, Tatyana Dyukova^c, Alla Savchuk^a, Sergei Balashov^d & Elena Korchemskaya^{a e}

^a Institute of Applied Optics, National Academy of Sciences, Kyiv, Ukraine

^b Zhytomir State University, Ukraine

^c Institute of Theoretical and Experimental Biophysics, Russian Academy of Sciences, Pushchino, Russia

^d University of California, Irvine, CA, USA

^e Institute of Physics, National Academy of Sciences, Kyiv, Ukraine

Version of record first published: 03 Mar 2011

To cite this article: Nikolai Burykin, Dmitriy Stepanchikov, Tatyana Dyukova, Alla Savchuk, Sergei Balashov & Elena Korchemskaya (2011): Real-Time Optical Information Processing Through the Use of Low-Saturable Absorption in Bacteriorhodopsin Films, *Molecular Crystals and Liquid Crystals*, 535:1, 140-147

To link to this article: <http://dx.doi.org/10.1080/15421406.2011.537966>

PLEASE SCROLL DOWN FOR ARTICLE

Full terms and conditions of use: <http://www.tandfonline.com/page/terms-and-conditions>

This article may be used for research, teaching, and private study purposes. Any substantial or systematic reproduction, redistribution, reselling, loan, sub-licensing, systematic supply, or distribution in any form to anyone is expressly forbidden.

The publisher does not give any warranty express or implied or make any representation that the contents will be complete or accurate or up to date. The accuracy of any instructions, formulae, and drug doses should be independently verified with primary sources. The publisher shall not be liable for any loss, actions, claims, proceedings, demand, or costs or damages whatsoever or howsoever caused arising directly or indirectly in connection with or arising out of the use of this material.

Real-Time Optical Information Processing Through the Use of Low-Saturable Absorption in Bacteriorhodopsin Films

NIKOLAI BURYKIN,¹ DMITRIJ STEPANCHIKOV,²
TATYANA DYUKOVA,³ ALLA SAVCHUK,¹ SERGEI
BALASHOV,⁴ AND ELENA KORCHEMSKAYA^{1,5}

¹Institute of Applied Optics, National Academy of Sciences, Kyiv, Ukraine

²Zhytomir State University, Ukraine

³Institute of Theoretical and Experimental Biophysics, Russian Academy of Sciences, Pushchino, Russia

⁴University of California, Irvine, CA, USA

⁵Institute of Physics, National Academy of Sciences, Kyiv, Ukraine

We have shown that the mechanism for a reversible anisotropic photoselection of bacteriorhodopsin (BR) molecules and a very small saturation intensity of a BR film allow for the blocking of any intensity feature from an image by just varying the intensity of a He-Ne laser beam without conventional frequency filters or rotation of an analyzer. It is found that the E204Q variant of BR offers additional valuable features. The photochemical cycle with a red-light absorbing O intermediate, $B \rightarrow M \rightarrow O \rightarrow B$, and a distortion of the grating profile due to the low-saturation absorption are responsible for a large initial peak sharpness of the dynamic holographic recording kinetics.

Keywords Bacteriorhodopsin; low-saturation absorption; real-time blocking; red-light absorbing O intermediate; reversible anisotropic photoselection

Introduction

Bacteriorhodopsin (BR), a light-driven proton pump and light-transducing photoreceptor protein from the microorganism *Halobacterium salinarum* [1], has appeared to be an outstanding photonic material for practical applications due to its unique properties and multifunctional photoresponse [2–6]. The BR proton pumping activity is, as known, accompanied by structural changes in the molecule which are reflected in spectral changes [7]. A large photochromic shift occurs during the photocycle of light-adapted BR. The initial form of BR, B, has an absorption peak at 570 nm, and the short-wave-absorbing intermediate M has an absorption peak at 412 nm. The time of the $B \rightarrow M$ transition is about 50 μ s. The spatial

Address correspondence to Elena Korchemskaya, Institute of Physics, National Academy of Sciences, Kyiv, Ukraine. E-mail: elkorch@iop.kiev.ua

resolution of BR films does not fall below 5000 lines/mm; images can be recorded on a film and erased for over a million cycles without degradation and require no external development.

The majority of applications of BR films use just B and M-states. However, it was recently shown that, under certain conditions, the red-light absorbing intermediates K in a wild-type (WT) BR film [8] and O in an E204Q BR film [9] can be formed in the BR films in the amounts sufficient for applications. The red-light absorption range is very attractive for practical applications due to the possibility to use compact inexpensive semiconductor lasers as a part of the device. The BR films have small saturation intensity due to high photosensitivity and decreased rates of the photocycle (as compared to those for a pigment in an aqueous suspension). The polymer films with natural WT BR show the saturation intensity of about 1 W/cm^2 for the photoinduced anisotropy. The chemically modified WT and some genetically mutated BR provide almost 4-fold increase in the photoanisotropic response and a 100-fold decrease in the saturation intensity [10]. It is usually thought that the saturation effects in materials were undesired features for the optical processing. In this work, we show that a combination of the low-saturable absorption with the photoinduced anisotropy in the chemically-modified D96 N BR film, as well as the presence of a considerable population of the red-light absorbing O-state in the E204Q BR film at high humidities along with the low-saturable absorption of this film, have a great potentiality for the real-time optical information processing.

Materials and Methods

Gelatin films made with WT BR, E204Q BR (in which the proton release complex is affected), and chemically modified D96 N BR (where the proton uptake pathway is affected) are fabricated as previously described [11]. The BR films have an optical density of about 2 at 570 nm. The thickness of the dried films at ambient humidity is approximately 70 μm .

Experimental setup for the real-time selective blocking of image feature of particular intensity. A He-Ne laser, $\lambda = 633 \text{ nm}$ (which excites the initial form, B, but not M) and a He-Cd laser, $\lambda = 442 \text{ nm}$, that predominantly excites the M intermediate are concurrently employed for the blocking of any intensity feature from an image (Fig. 1). The film is mounted between a crossed polarizer and analyzer. The plane of polarization of the He-Ne laser beams is oriented at 45° with respect to the He-Cd laser beam. The mirrors M1, M2 have a 70-% transparency at 442 nm and a 70-% reflectivity at 633 nm. An object pattern having an inhomogeneous spatial-intensity distribution can reside in the object beam of a He-Ne laser. Linearly polarized red light performs an anisotropic photoselection of BR molecules in the B form. Linearly polarized blue light serves as a testing beam and simultaneously runs some anisotropic photoselection of molecules in the M form [10]. Red light is then cut with a blue filter, and the processed pattern is imaged on a CCD camera. The He-Cd laser beam and the controlling He-Ne laser beam have diameters of about 1 and 2 mm, respectively. They are expanded by a twenty-power telescope in the He-Cd laser beam and a ten-power one in controlling He-Ne laser beam. Next, the central fragments of these He-Cd and He-Ne laser beams are cut with diaphragms; they present relatively homogeneous spatial-intensity distributions of about 4 mm in diameter. At the location of image features with intensities equal

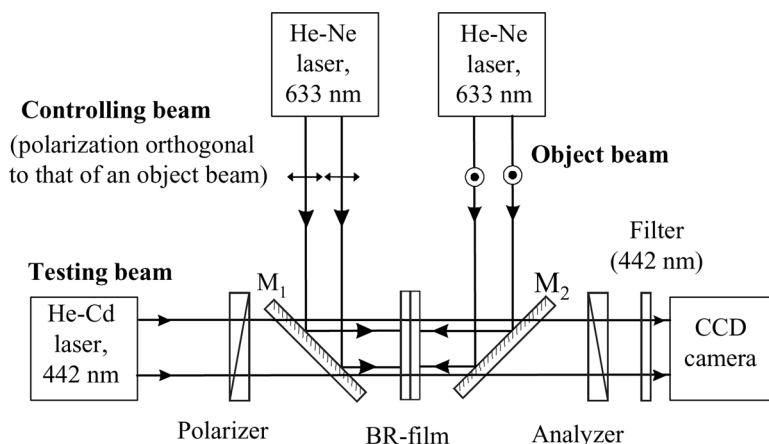


Figure 1. Schematic for the experimental setup for the real-time selective blocking of any intensity feature from an image by applying the photoinduced anisotropy to a BR film.

to that of a controlling He-Ne laser beam, molecules in the initial B form equally absorb 633-nm light regardless of their angular orientation. Thus, the photoinduced anisotropy locally disappears in the BR film.

Humidity-holographic technique. Mounting a small cell with a BR film inside the holographic setup [12] allowed us to perform holographic measurements on a film at a desired humidity over long periods of time. It is important since features of the film depend on humidity (water content). A cw He-Ne laser with $\lambda = 633$ nm was used for both the holography grating recording and probing the time course of the recording. The beam from a recording He-Ne laser is split into two beams I_1 and I_2 of the same intensity $I_{1,2} = 200$ mW/cm². These two plane waves were recombined with an angle of 3° between them. Under these conditions, the thin transmission grating with a spacing of approximately 40 μ m is recorded in the BR film. A probe beam of the same wavelength, but not coherent with the recording beams with an intensity of 8 mW/cm², was directed on the BR film at a nearly Bragg angle. The kinetics of the symmetric first-order diffracted probe beams were measured by a digital storage oscilloscope TDS2014 (Tektronix).

Results and Discussion

For the real-time selective blocking of an image feature having particular intensity, chemically modified D96 N BR is used. In the WT and D96 N BR films, a photochemical cycle at humidity values of 60–99% can be approximately described as inter-conversions of just two states, $B \leftrightarrow M$: the initial state of BR, B, and the short-wave-absorbing intermediate M. Other intermediates are formed, but are not accumulated. The D96 N BR film with chemical additions demonstrates a considerably prolonged M lifetime and a substantial gain in the bleaching efficiency and, hence, in photoanisotropic response [10].

The magnitude of an output intensity of a testing He-Cd laser beam depends on the anisotropy induced in the BR film, as well as on the input intensity of a He-Cd laser beam. The BR films are known to have a strong nonlinear intensity dependence

of a photoanisotropic response [4,5,10]. At a fixed intensity of the input He-Cd laser beam, the photoinduced anisotropy reaches a maximum for a definite intensity of an object He-Ne laser beam (Fig. 2). The further increase in the object He-Ne laser beam intensity disturbs the maximum anisotropic distributions of B and M forms, since almost all BR molecules are converted into the intermediate M regardless of their angular orientation. At a fixed intensity of the object He-Ne laser beam, an increase of the input intensity of a He-Cd laser beam also decreases the anisotropy, since a considerable number of BR molecules in M can be returned to the initial form B regardless of their angular orientation. Similar to the dynamics of B and M populations, the photoinduced anisotropy is defined by a relation between the intensities of He-Ne and He-Cd lasers. In our experiments, the output intensity of a He-Cd laser beam of $13 \mu\text{W}/\text{cm}^2$ is obtained at an input intensity of $2.5 \text{ mW}/\text{cm}^2$, which suits well for the processing of an object information having average intensity features of about $10 \text{ mW}/\text{cm}^2$. For comparison, in the case where a He-Ne laser beam is used also as a testing beam (B-type anisotropy), the maximum value of the output intensity of a testing He-Ne laser beam of $2 \mu\text{W}/\text{cm}^2$ is reached at the intensity of an object He-Ne laser beam of $2 \text{ mW}/\text{cm}^2$. The further increase in the intensity of testing and object He-Ne beams causes a decrease in the anisotropy.

The overall blocking of high-intensity features from an object, as well as the edge enhancement, can be reached by increasing the intensity of an object He-Ne laser beam to the saturation. For a chemically modified D96N BR-film, the optimum intensity to induce an anisotropy is about $10 \text{ mW}/\text{cm}^2$ (Fig. 2, curve 3). At the intensity of a He-Ne laser beam exceeding $200 \text{ mW}/\text{cm}^2$, the BR-film appears to be in a transient isotropic state, and the photoinduced anisotropy decays. For the purposes of the simplest demonstration of the potentiality of a combination of the

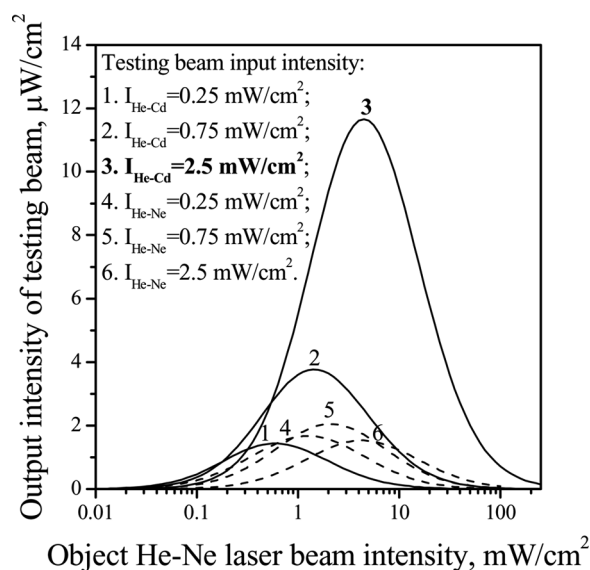


Figure 2. Calculated output intensity of both a testing He-Cd laser beam to induce the B-M-type anisotropy (solid curves) and a testing He-Ne laser beam to induce the B-type anisotropy (dashed curves) as a function of the object He-Ne laser beam intensity made at various input intensities of the testing beams $I_{\text{He-Cd}}$ and $I_{\text{He-Ne}}$.

low-saturable absorption with the photoinduced anisotropy, it is convenient to use a Gaussian beam itself (radius $r = 1$ mm) residing in the object He-Ne laser beam. For this case, the telescope and the diaphragm are removed from the object beam.

A mechanism for the reversible anisotropic photoselection of BR molecules [4,10] allows for the real-time selective blocking of an image feature having a particular intensity. An additional controlling He-Ne laser beam with a polarization orthogonal to that of an object beam is used for this purpose (Fig. 1). At the location of an image feature, whose intensity equals that of the controlling He-Ne laser beam, BR molecules in the initial form B are equally capable to absorb red light regardless of their angular orientation. Thus, the photoinduced anisotropy locally decays in the BR film. Respectively, this image feature is not transmitted through the system of a crossed polarizer and analyzer with the BR film. The results of calculations of the spatial-intensity transition of a Gaussian beam at various intensities of a controlling He-Ne laser beam is shown in Figure 3a. By choosing an appropriate intensity level of a controlling He-Ne laser beam, it is possible to block an image feature having a particular intensity. At the location of image features, whose intensities are not equal to that of a controlling He-Ne laser beam, the anisotropy also somewhat declines so that the calculated contrast ratio becomes 150:1. A signal outside the profile of a Gaussian beam derives from the fact of a larger diameter of a controlling He-Ne laser beam as compared to that of the object Gaussian beam. The experimental demonstration of the real-time selective blocking of a feature having a particular intensity from the object Gaussian beam by varying the intensity of a controlling He-Ne laser beam is shown in Figure 3b. Thus, a combination of the photoinduced anisotropy with the low-saturable absorption in a chemically modified D96 N BR film allowed for the blocking of any intensity feature from an image without conventional frequency filters.

Kinetics of holographic grating recording under different conditions in WT and E204Q BR. A comparative study of the transmittance and holographic recording kinetics at 633 nm and a humidity of 60–99% is performed on E204Q and WT BR gelatin films. Similar to the light-adapted WT BR film [12], the grating recording kinetics in the E204Q BR film consists of two stages: an initial increase to a maximum value (a peak) followed by a decrease to a steady state (Fig. 4). The diffraction efficiency kinetics depends on the spatial grating profile. The spatial profile of the recording grating in a BR film varies with the recording time due to the low-saturation absorption [13]. At the maximum value of the diffraction efficiency, a spatial grating profile is close to a sinusoidal one, and then a distortion of the grating profile occurs, causing a decrease in the diffraction efficiency.

At a humidity of 60%, the shapes of the grating recording kinetics in the WT and E204Q BR films match almost exactly (Fig. 4a). The ratio between the peak and steady-state values for the 633-nm probe beam equals 2. At a humidity of 98%, the grating recording kinetics in the WT and E204Q BR films are considerably different (Fig. 4b). For the 633-nm probe beam, the ratio between the peak and steady-state values is 1.5 for the WT BR film, whereas it is 5.4 for the E204Q BR film. We suggest that a two-state photocycle model, $B \leftrightarrow M$, which seems adequate for a humidity of 60%, should be substituted for a three-state model $B \rightarrow M \rightarrow O \rightarrow B$ for higher humidity values, especially for the E204Q mutant, where the O intermediate is accumulated [14]. The intermediate O has an absorption peak at 640 nm. The calculation in terms of the time constants for the E204Q BR photocycle shows

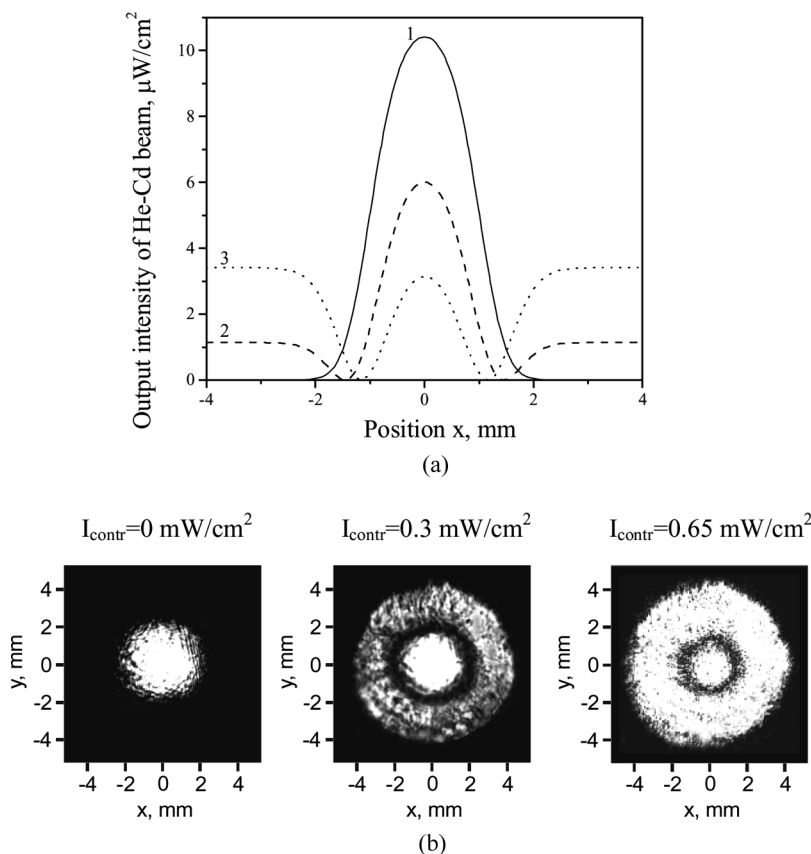


Figure 3. (a) The calculated curves of the spatial intensity transition of a Gaussian beam, $r = 1$ mm for various intensities of a controlling He-Ne laser beam: $I_{\text{contr}} = 0$ (curve 1), 0.3 (curve 2), and 0.65 mW/cm^2 (curve 3). The intensity of the object beam of a He-Ne laser at the center ($x = 0, y = 0$) of a Gaussian beam $I_0 = 2.5 \text{ mW/cm}^2$; (b) Experimental demonstration of the selective blocking of a feature having a particular intensity from the object Gaussian beam under calculated conditions.

that, in a steady-state at a humidity of 60%, the majority of BR molecules presents the M intermediate. In a steady-state at a humidity of 98%, a part of BR molecules is in the M intermediate, and a part is in the O intermediate. During the initial peak, the O intermediate population is yet insignificant, but it is accumulated with time and causes a decrease in the transmittance of a red probe beam. Upon probing the E204Q BR film by a red laser beam at high humidities, a steady-state in the diffraction efficiency kinetics shows the extra-decline due to the formation of the O_{640} intermediate in the last part of a photocycle. This results in a significant gain in the initial peak sharpness (decay to a steady state). This particular feature could be extremely useful for the development of a novelty filter and the detection of an object rapid movement.

In conclusion, we have demonstrated the potentialities for applications of a photoinduced anisotropy combined with the low-saturable absorption in BR films for a nonlinear spatial light modulation. For this purpose, He-Ne and He-Cd lasers

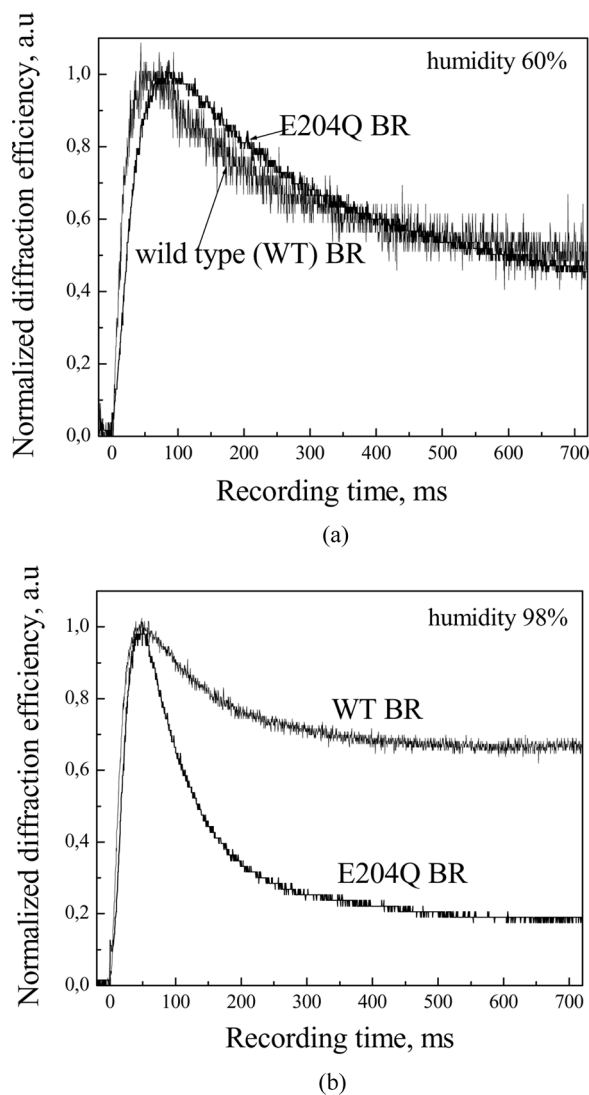


Figure 4. Comparison of the normalized diffraction efficiency kinetics in the WT and E204Q BR films at 60% (a) and 98% (b) humidity values upon recording with a low-intensity cw He-Ne laser.

were employed here; it is also possible to employ low-intensity diode lasers. The mechanism for a reversible anisotropic photoselection of BR molecules along with a very small saturation intensity of chemically modified D96 N BR films allows for the blocking of any intensity feature from an image by just varying the intensity of a He-Ne laser beam without conventional frequency filters or the rotation of an analyzer. An important advantage of the use of the B-M-type anisotropy is a considerable gain in the contrast ratio, since the blocking of high-intensity features is based not only on the anisotropy decay, but also on an increase of the absorption coefficient at the testing with a He-Cd laser beam.

It is found that, in the E204Q BR gelatin film at high water content (a humidity of 98%), about 80% of BR molecules undergo the photocycle involving the red-light absorbing O intermediate, $B \rightarrow M \rightarrow O \rightarrow B$. This particular pathway is responsible for a large transient change in the diffraction efficiency of the dynamic holographic recording on the E204Q BR film. This feature is potentially useful in certain applications. For example, it can be implemented as a novelty filter. The results can offer several advantageous strategies in the optical processing field and the development of photochromic media.

Acknowledgment

The present research is supported in part by Award No. UB2-2427-KV-02 of the U.S. Civilian Research & Development Foundation for the Independent States of the Former Soviet Union (CRDF; to N.B., D.S., S.B., and E.K.).

References

- [1] Oesterhelt, D., & Stoeckenius, W. (1973). *Proc. Natl. Acad. Sci. U. S. A.*, 70, 2853.
- [2] Wise, K. J., Gillespie, N. B., Stuart, J. A., Krebs, M. P., & Birge, R. R. (2002). *Trends Biotechnol.*, 20, 387.
- [3] Seitz, A., & Hampp, N. (2000). *J. Phys. Chem. B*, 104, 7183.
- [4] Korchemskaya, E., Stepanchikov, D., & Burykin, N. (2001). In *Bioelectronic Applications of Photochromic Pigments*. Der, A. & Keszthelyi, L. (Eds.), IOS Press: Amsterdam, p. 74.
- [5] Huang, Y., Siganakis, G., Moharam, M. G. J., & Wu, S.-T. (2004). *Optics Letters*, 29, 1933.
- [6] Ferrari, J. A., Flores, J. L., Perciante, C. D., & Frins, E. (2009). *Applied Optics*, 48, 3570.
- [7] Balashov, S. P., & Lanyi, J. K. (2006). In *Microbial Bionanotechnology*, Rehm, B. (Ed.), Horizon Press: London, p. 339.
- [8] Der, A., Valkai, S., Fabian, L., Ormos, P., Ramsden, J. J., & Wolff, E. K. (2007). *Photochemistry and Photobiology*, 83, 1.
- [9] Stepanchikov, D., Burykin, N., Dyukova, T., Ebrey, T. G., Balashov, S. P., & Korchemskaya, E. (2006). *Functional Materials*, 13, 669.
- [10] Korchemskaya, E., Stepanchikov, D., & Dyukova, T. (2000). *Optical Materials*, 14, 185.
- [11] Dyukova, T., & Lukashev, E. (1996). *Thin Solid Films*, 283, 1.
- [12] Korchemskaya, E., Burykin, N., Bugaychuk, S., Maksymova, O., Ebrey, T., & Balashov, S. (2007). *Photochemistry and Photobiology*, 83, 403.
- [13] Bugaychuk, S., Korchemskaya, E., & Burykin, N. (2002). *Ukr. J. Phys. Opt.*, 3, 27.
- [14] Brown, L. S., Sasaki, J., Kandori, H., Maeda, A., Needleman, R., & Lanyi, J. K. (1995). *J. Biol. Chem.*, 270, 27122.